Published in Physical Review Letters 90, issue 196804, 1-4, 2003
which should be used for any reference to this work

Electronic Structure of the YH_3 Phase from Angle-Resolved Photoemission Spectroscopy

J. Hayoz,[1,*] C. Koitzsch,[2] M. Bovet,[1] D. Naumović,[1] L. Schlapbach,[1] and P. Aebi[2]
[1]*Département de Physique, Université de Fribourg, Pérolles, CH-1700 Fribourg, Switzerland*
[2]*Institut de Physique, Université de Neuchâtel, CH-2000 Neuchâtel, Switzerland*

Yttrium can be loaded with hydrogen up to high concentrations causing dramatic structural and electronic changes of the host lattice. We report on angle-resolved photoemission experiments of the Y trihydride phase. Most importantly, we find the absence of metal *d* bands at the Fermi level and a set of flat, H-induced bands located at much higher binding energy than predicted, indicating an increased electron affinity at H sites.

Recently, switchable optical properties of metal hydrides at ambient pressures and temperatures have attracted strong interest [1]. For trivalent Y, for instance, up to three H atoms can be absorbed. The dihydride is even a better metal than Y itself but during the transition to the trihydride phase it turns from shiny metallic to transparent and insulating. With H a proton and an electron are introduced to the metal host. This results in doping the host material. Different models have been proposed to explain this spectacular metal-insulator transition (MIT). However, the behavior of H in such hydrides is still under debate.

State-of-the-art *ab initio* local density approximation (LDA) calculations do not reproduce the optical gap necessary to explain the transparent state in the trihydride phase unless additional symmetry lowering is considered by displacing H atoms away from positions given by the HoD_3 structure of YH_3 [2]. Other models [3,4], based on strong electron correlations, have been proposed to explain the MIT. Ng *et al.* [3] studied the effect of correlations on the bandwidth of H-induced states. Hydrogen is present in the form of H^- [5,6], where one electron is taken from the metal host. The two electrons on H^- are strongly correlated and the essence of the result of Ng *et al.* [3] is that the opening of the band gap is due to a correlation-induced band narrowing.

The model of Eder *et al.* [4] is based on the observation that the radius of H is very sensitive to the occupation number. The two electrons on H^- are correlated but with drastically different radii around the proton. This results in a so-called breathing mode and a local singletlike bound state with one electron on the proton and the other on the neighboring metal orbitals. Already at the mean field level this introduces a significant correction to the potential at the H site, effectively increasing the electron affinity, lowering the H band, and opening the gap.

On the other hand, very recent *GW* calculations [7,8] demonstrate the formation of a sufficient gap to explain the MIT without the need for strong electron correlations. Rather, these calculations indicate that the gap opening is described as in normal semiconductors. For semiconductors LDA does not produce the correct gap, whereas the self-energy corrections included in the *GW* calculations are able to account for this deficiency.

Indeed, detailed angle-resolved photoemission (ARPES) experiments are needed to favor one or the other model. However, practically all previous work on metal hydrides has been done on polycrystals and/or on samples that are capped with a protective Pd layer. In order to perform ARPES experiments, uncapped single-crystalline material is needed. Furthermore, preparation has to take place *in situ* since Y is extremely reactive.

Here we present, to our knowledge, the first ARPES data on the trihydride phase of uncapped single-crystalline films. We find that the overall bandwidth of the Y trihydride phase agrees with LDA calculations. However, a set of flat bands is observed with significantly higher binding energy, a fact that argues in favor of the model proposed by Eder *et al.* [4].

Experiments were performed in a VG ESCALAB Mk II spectrometer with motorized sequential angle-scanning data acquisition [9]. ARPES measurements were performed with monochromatized He Iα ($h\nu =$ 21.2 eV) at room temperature [10]. The energy resolution is 35 meV. Single-crystalline Y hydride films were grown on a W(110) single crystal. Details of the preparation and the careful characterization of the crystal and electronic structure and the calibration of the H concentration have been described elsewhere [11,12]. In brief, this setup allows one to prepare clean, single-crystalline rare-earth hydride films using H pressures up to 1.3 bars. It combines a high-pressure reaction cell with a custom made hydrogen purification system based on a Pd-24%Ag permeation tube and a sorption pump. The results presented here are taken from 200 Å thick, well-ordered [13] single-crystalline films [11] in the trihydride phase [14]. The H composition is determined via photoelectron diffraction and x-ray photoelectron spectroscopy (not shown) to be $YH_{2.9}$ [11].

Band structure calculations using the full-potential linearized augmented plane-wave method [15] within the generalized-gradient approximation [16] have been

performed for comparison with the experiments. Calculations were performed for the HoD_3 structure with space group 165 ($P\bar{3}c1$). The lattice parameters used for the YH_3 calculation were $a = b = 6.34$ Å and $c = 6.6$ Å. A total of 485 k points within the irreducible wedge of the Brillouin zone (BZ) were considered for the self-consistency cycles and convergence was reached to within 0.1 mRy.

Figure 1 shows ARPES data measured along two high symmetry directions of the surface BZ. The situation in reciprocal space is illustrated in Fig. 2 where the surface BZ (left) and a cut through the extended bulk BZ containing the Γ, *A, H, L, M, K* high symmetry points (right) is shown. YH_3 with the HoD_3 structure consists of a $(\sqrt{3} \times \sqrt{3}) - R30°$ reconstruction with respect to the hexagonal Y lattice, i.e., the unit cell has a and b vectors which are $\sqrt{3}$ times longer and rotated by 30°. Therefore the YH_3 BZ is smaller and rotated accordingly (Fig. 2).

Inspecting the experimental spectra (Fig. 1) a similar behavior is observed for both directions. The dispersion appears relatively weak and the electronic states do not reach the Fermi level (E_F) or 0 eV binding energy, which is indicative for a gap. The d states that are present in Y ($[Kr]4d^15s^2$) and YH_2 (not shown) have disappeared [17]. Five dispersing features are easily discernible and are labeled from 1 to 5. A broad almost dispersionless maximum between 5.5 and 8.3 eV (shaded area) persists for all angles, respectively, k points. At first sight one is tempted to interpret the fact that the dispersion is weak and the spectral features are broad as caused by strong electron correlations and self-energy effects.

However, taking a closer look reveals a different point of view. In Fig. 3 the result of our band structure calculation of YH_3 in the HoD_3 structure is displayed. As mentioned above, the approach using LDA does not show a gap. The calculation presented here is in good agreement with the results of Kelly *et al.* [2]. We notice that there are many bands. This is a consequence of the large real-space unit cell of the HoD_3 structure containing 24 atoms including six Y atoms and 18 H atoms in the unit cell. The important point to notice here is that there is a set of rather flat, H-induced bands (as deduced from a band character analysis) between 1.8 and 4.6 eV (dark shaded area) extending over the whole bulk BZ. Such a set of flat bands naturally gives rise to a high density of states (DOS) in this energy region. This leads to the interpretation of the broad, high intensity features in the experiment (shaded area in Fig. 1) as due to these flat bands [18]. The energy width of the region in the experiment agrees well with the energy interval of the flat bands in the band structure calculation. The only difference is that the experimental bands occur at a 3.7 eV greater binding energy.

In order to obtain a more detailed comparison we use a gray scale representation of both the experimental data and the calculated band structure. Figure 4 displays the results along the $\bar{\Gamma}\bar{K}$ direction. For the experimental data (left) the second derivative of the spectra of Fig. 1 has been plotted as a function of wave vector parallel to the surface ($k_{\|}$). The reason for plotting the second derivative is to flatten the spectra and to accentuate the dispersing features. The calculation (right) follows the free-electron final-state (FEFS) wave vectors drawn in Fig. 2 [19]. The locations of the flat bands are marked by shading the energy scales in both the experiment and the calculation

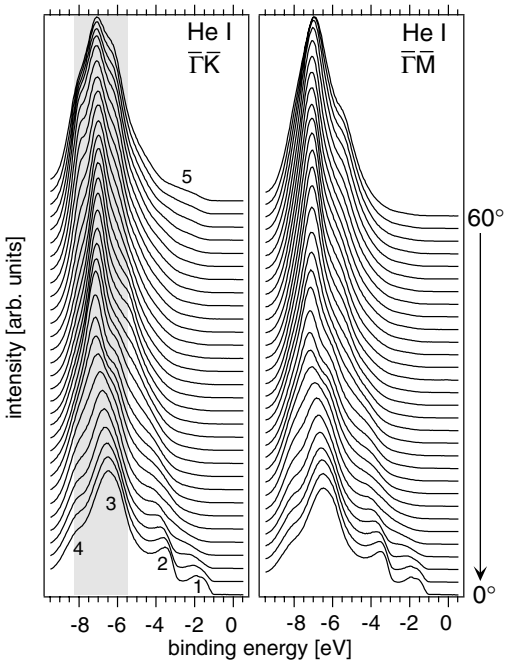

FIG. 1. Energy distribution curves taken along the $\bar{\Gamma}\bar{K}$ (left) and $\bar{\Gamma}\bar{M}$ (right) directions of the surface BZ (see Fig. 2), collecting spectra up to 60° off-normal emission. Normal emission (0°) corresponds to $\bar{\Gamma}$; the $\bar{K}$ and $\bar{M}$ points are reached approximately at 17° and 15° off-normal emission, respectively, for 0 eV binding energy. Mapping into k space is shown in Fig. 4. A shaded area marks weakly dispersing, broad spectral features (see text).

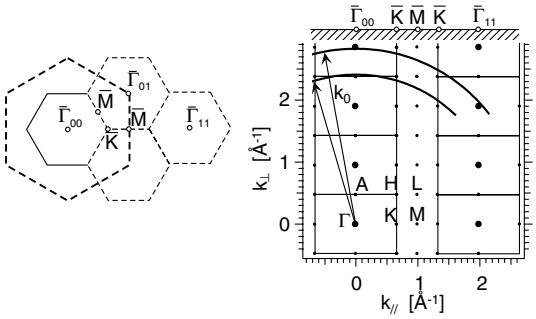

FIG. 2. Situation in k space. Left: The surface BZ for the HoD_3 structure with high symmetry points. The large hexagon represents the surface BZ for the Y sublattice. Right: Section across the bulk BZ containing the Γ, *A, H, L, M, K* high symmetry points. Spherical segments indicate the k-space region probed within the FEFS approximation used for the calculation in Fig. 4.

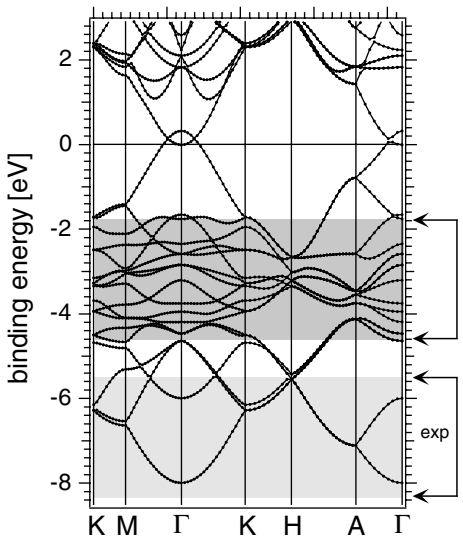

FIG. 3. LDA based band structure calculation for the HoD_3 structure. Indicated is the region (dark shading) of flat, H-induced bands and the corresponding region (light shading) where the experiment (Fig. 1) shows a high density of states (see text).

where they occur with a 3.7 eV smaller binding energy. We have to note that the experiments do not probe the path along high symmetry directions in the *bulk* BZ. Rather, the experiment follows a circlelike path as indicated in Fig. 2. At $k_{\|}$ values between 0.7 and 1 $Å^{-1}$ (see Fig. 2, right) we pass the region of *K* and *M* points, and we can compare Fig. 4 with the *KM* dispersion of Fig. 3. The bands are concentrated around a narrow energy range and the discrepancy between experiment and calculation induced by the band shift is evident. In addition, we can identify the bands labeled 1 to 5 as already indicated in Fig. 1. These labels, 1–5, in both figures have the same relative positioning, but in the calculation they are rigidly shifted upwards by $\approx$ 1.5 eV. At this point we have to

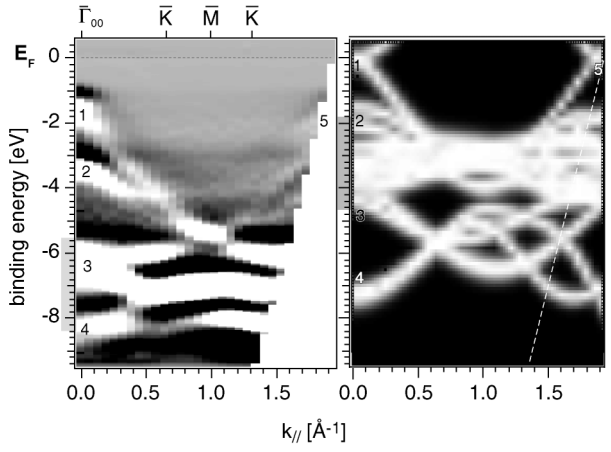

FIG. 4. Second derivative of spectra from Fig. 1 mapped into *k* space using gray scale intensity coding with high intensity in white (left). Model calculation using the FEFS approximation (right) (see text).

note that the agreement of relative positions is extremely good taking into account the fact that we use the FEFS approximation. Labels 1, 2, and 5 can directly be attributed to each other. The difficulty appears for labels 3 and 4 since this is where the downward shift of the flat bands affects the comparison. Looking at the right side of Fig. 4 (calculation) we see the flat bands between labels 2 and 3 as an accumulation of almost horizontal lines between 1.8 and 4.6 eV binding energy. In the experiment, as explained above, these flat bands appear between 5.5 and 8.3 eV binding energy. In fact, they come to lie on top of labels 3 and 4 and therefore obscure the direct comparison between experiment and calculation in this energy range.

Comparing our experiments with the LDA calculation shows that the overall band width compares well. The differences are a rigid shift of approximately 1.5 eV and the position of the flat bands. However, a detailed comparison of different bands and their relative positions depends on the validity of the FEFS approximation. Therefore we cannot, at present, give a robust statement about the exact position of the top of valence band (label 1, Fig. 4, left) and, as a consequence, about the size of the gap. This depends on the exact location in the component of the wave vector perpendicular to the surface, $k_{\perp}$. On the other hand, the difference in the position of the flat bands is independent of this approximation since the flat bands extend over the whole BZ as seen from experiment (Fig. 1) and theory (Fig. 3). In a way the situation is very favorable for the interpretation. The spectra in Fig. 1 are very similar along the two different directions of the BZ. This indicates, in particular, that the broad feature between 5.5 and 8.3 eV binding energy is characteristic for the phase and persists in large parts of the BZ. At the same time the LDA band structure calculation of Fig. 3 shows the flat bands between 1.8 and 4.6 eV extending along all the high symmetry directions, again indicating that they are characteristic for the phase and persist in large parts of the BZ. Using this observation and attributing the flat bands to the high DOS, i.e., the broad high intensity spectral feature, we affirm the downward shift of flat bands. That the overall bandwidth is in good agreement with LDA also follows from comparing the experimental spectra (Fig. 1) and the band structure calculation (Fig. 3). In particular, the bandwidth extends down to below 8 eV binding energy.

It is interesting now to compare with theoretical models. At first we look at the *GW* calculations. In the study of Miyake *et al.* [7] the gap opens due to a shifting up of the conduction bands, whereas in the case of van Gelderen *et al.* [8] the gap opens because of both shifting up of the conduction bands and shifting down of valence bands. Otherwise, the quasiparticle wave functions are practically identical to the LDA wave functions and there is basically a one-to-one correspondence between the bands of the LDA and *GW* band structures. The total bandwidths do not differ significantly as well. From our experiments we conclude that the overall bandwidth is well

reproduced by LDA and *GW* calculations. However, the high binding energy of the flat bands is not reproduced. Even the downwards shift of the valence bands ($\approx$ 1 eV) in the case of van Gelderen *et al.* [8] is not sufficient and does not account for the *relative* shift of certain bands.

Clearly, the good agreement of the overall bandwidth with the LDA calculations is in contrast to the model of Ng *et al.* [3] where strong electron correlations induce a band narrowing. However, we cannot exclude that individual bands are subject to narrowing. The reason is that from the experimental data, due to the large number of bands, it is not possible to identify every individual band. The width of the experimentally observed spectral features is not resolution limited and might be explained either by self-energy effects or also by a relatively high mobility of H atoms and defects due to the substoichiometry of the films. Furthermore, there is still debate on whether the HoD_3 structure really corresponds to the one for YH_3 [20,21].

Finally, we compare our results to the model by Eder *et al.* [4]. The dependence of the occupation number of electrons on the H site is incorporated in their model Hamiltonian by having a novel hopping integral. The resulting singletlike bound state is manifest via increasing the binding energy of the H states. Contrary to the treatment of Ng *et al.* where the result is a narrowing of bands, Eder *et al.* [4] predict a shift of the potential at the H site *retaining* the large H bandwidth.

It is now very tempting to interpret our data, showing a shift of bands towards higher binding energy, in terms of such an additional potential on H sites. Observing Fig. 3 it appears that only the set of flat bands is strongly shifted down, whereas the others, covering the full bandwidth, are consistent with the *GW* approach. This might be interpreted in the sense that the bands within the set of flat bands have a more localized character and therefore are stronger affected by the singletlike bound state. However, a detailed comparison of how different bands are affected is not possible since a realistic band structure for the HoD_3 structure is not available within Eder's model Hamiltonian.

In conclusion, we have performed ARPES experiments on single-crystalline films of Y in the trihydride phase. A comparison with LDA calculations shows a good agreement of the overall bandwidth. No significant band narrowing is observed although a narrowing of individual bands cannot be excluded. However, a set of H-induced, flat bands is identified in the experiment with a binding energy $\approx$ 3.7 eV higher than in the calculation. Furthermore, based on the FEFS approximation, we infer a rigid shift of the valence band towards higher binding energy by more than 1 eV which is consistent with *GW* calculations [8] and the opening of a gap. The downwards shift of flat bands supports the model proposed by Eder *et al.* [4] predicting a shift of the potential at the H site and *retaining* the broad H band.

Skillful technical assistance was provided by E. Mooser, O. Raetzo, R. Schmid, O. Zosso, Ch. Neururer, and F. Bourqui. This project has been supported by the Fonds National Suisse de la Recherche Scientifique.

*Present address: SenTec AG, Ringstrasse 39, CH-4106 Therwil BL, Switzerland.

[1] J. N. Huiberts *et al.*, Nature (London) **380**, 231 (1996).
[2] P. J. Kelly, J. P. Dekker, and R. Stumpf, Phys. Rev. Lett. **78**, 1315 (1997).
[3] K. K. Ng *et al.*, Phys. Rev. Lett. **78**, 1311 (1997).
[4] R. Eder, H. F. Pen, and G. A. Sawatzky, Phys. Rev. B **56**, 10 115 (1997).
[5] F. J. A. den Broeder *et al.*, Nature (London) **394**, 656 (1998).
[6] M. Rode *et al.*, Phys. Rev. Lett. **87**, 235502 (2001).
[7] Takashi Miyake *et al.*, Phys. Rev. B **61**, 16 491 (2000).
[8] P. van Gelderen *et al.*, Phys. Rev. Lett. **85**, 2989 (2000).
[9] J. Osterwalder *et al.*, Phys. Rev. B **44**, 13 764 (1991); D. Naumović *et al.*, Phys. Rev. B **47**, 7462 (1993).
[10] Th. Pillo *et al.*, J. Electron Spectrosc. Relat. Phenom. **97**, 243 (1998).
[11] J. Hayoz *et al.*, J. Vac. Sci. Technol. A **18**, 2417 (2000).
[12] J. Hayoz *et al.*, Phys. Rev. B **58**, R4270 (1998).
[13] The films exhibit well-defined low energy electron diffraction spots according to the hexagonal arrangement of Y in the HoD_3 structure. The H-induced superstructure does not appear since H is a weak scatterer.
[14] E_F calibration is important since the H_3 phase is insulating and charging effects could shift the spectra; that this is not the case has been verified by blowing up the zero-binding energy region up to the point where the Fermi-Dirac distribution onset becomes visible.
[15] P. Blaha, K. Schwarz, and J. Luitz, WIEN97, Vienna University of Technology. [Improved and updated UNIX version of the original copyrighted WIEN code, P. Blaha, K. Schwarz, P. Sorantin, and S. B. Trickey, Comput. Phys. Commun. **59**, 399 (1990)].
[16] J. P. Perdew, K. Burke, and M. Ernzerhof, Phys. Rev. Lett. **77**, 3865 (1996).
[17] J. Hayoz, Ph.D. thesis, University of Fribourg, Switzerland, 1999.
[18] DOS calculations (not shown) indicate, indeed, a peaked DOS around -3 eV (region of flat bands). Matrix elements should not change strongly over the binding energy range (since all bands below E_F have almost exclusively H character) and the interpretation of the spectral intensity in terms of DOS should be valid.
[19] The gray scale levels of the calculation are determined by checking energy conservation with respect to the FEFS; i.e., perfect energy conservation appears in white. An inner potential of 10 eV and a work function of 3 eV have been assumed. No matrix elements are considered.
[20] T. J. Udovic *et al.*, Phys. Rev. B **61**, 12 701 (2000).
[21] P. van Gelderen, P. J. Kelly, and G. Brocks, Phys. Rev. B **63**, 100301 (2001).